Current-driven vortex dynamics in a periodic potential

Y. Yuzhelevski and G. Jung*
Department of Physics, Ben Gurion University of the Negev, P.O. Box 653, 84105 Beer-Sheva, Israel

C. Camerlingo and M. Russo
Consiglio Nazionale delle Ricerche, Istituto di Cibernetica, 85100 Arco Felice (NA), Italy

M. Ghinovker and B. Ya. Shapiro
Center of Superconductivity, Department of Physics, Bar-Ilan University, 52900 Ramat-Gan, Israel
(Received 8 February 1999)

Quasi-Josephson effects due to coherent vortex motion in artificial reversible periodic potential structures in high-T_c superconducting thin films have been investigated. Periodic pinning conditions have been created by applying a magnetic tape containing a prerecorded harmonic signal to the surface of high quality $Y_1Ba_2Cu_3O_{7-\delta}$ thin films. Application of the periodic pinning enforces coherence in current-driven motion of Abrikosov vortices in wide and short macrobridges and leads to the appearance of Josephson-like effects manifesting themselves in series of self-induced current steps on the current-voltage characteristics. The equation of motion for vortices flowing across periodic potential structures is analogous to the phase equation for low-capacitance classical Josephson junctions. The perturbation solutions of this equation contain resonant Shapiro-like self-steps resulting from the locking of the frequency at which vortices are created at the sample borders to the resonant frequencies of the vortex system. Self-resonant frequencies are set by the characteristic time of flight across the sample width and across the period of the applied potential. Voltages of the self-induced current steps have been found to scale with inverse of the characteristic length corresponding to the magnetic period and/or to the sample half-width, consistently with the theoretically derived relations. Experimental data indicate that vortices move in large bundles containing several thousands of flux quanta. The temperature dependence of the step voltages can be ascribed to changes in vortex velocity due to the temperature-dependent viscosity factor. [S0163-1829(99)01334-X]

I. INTRODUCTION

Classical Josephson quantum coherence effects with pure sine current-phase relationship persist only in very small weak links having dimensions of the order of the superconducting coherence length of the material from which they are made.[1–5] Voltage states observed in experimentally achievable high-T_c superconductor (HTSC) bridges, despite some claims in the literature, are not related to the Josephson effects but to the dissipation caused by the motion of Abrikosov vortices. With increasing transport current large weak links (macrobridges) became unstable with respect to vortex formation. Bundles of vortices of opposite sign nucleate at strip borders, move toward the bridge center, and annihilate. In bridges smaller than the effective penetration depth of magnetic field repulsive forces between equally oriented vortices and attractive forces between oppositely oriented ones cause highly coherent motion of vortex bundles. Coherent flow of vortices results in the appearance of Josephson-like effects, closely resembling phenomena seen in classical Josephson junctions.[2,3] One observes magnetic modulation of the critical current and Shapiro dc current steps on I-V characteristics of microwave irradiated samples.[4–10] The coherent nature of vortex based Josephson-like effects was most convincingly confirmed by direct detection of microwave emissions by coherently flowing vortices.[10–12]

Josephson-like effects related to coherent vortex motion were studied extensively already in low-T_c superconducting weak links, see, e.g., Refs. 4–8. The phenomenon was most pronounced in weak links made out of short coherence length materials, such as A-15 (Refs. 4–6) or disordered ion-implanted superconductors.[7] It was found that with increasing size of the bridge, vortices start to nucleate and penetrate the bridge simultaneously at different positions along its edges. In this situation, nonhomogeneity and intrinsic pinning became more important and led to differences of velocities along different channels of vortex motion. As a consequence, the coherence in vortex motion breaks down with increasing link size and very large bridges behave like ordinary superconducting films.

A recent decade of intensive investigations of HTSC's resulted in enormous progress in our understanding of the properties of vortex matter in type-II superconductors.[13] Among many experimental techniques, artificial pinning proved to be an extremely useful tool in studies of vortex dynamics. Enforcement of artificial pinning is capable of changing in a significant degree the electromagnetic properties of vortex matter. A common way of changing the pinning properties consists of exposing samples to electron, ion, or neutron irradiation, capable of introducing additional quenched disorder to the specimen. Recently the general interest shifted towards effects of ordered artificial periodic pinning structures.[14–20] Interaction of vortex matter with periodic pins can be seen as an excellent laboratory model of a general class of nonlinear systems. Current-driven vortices interacting with periodic pins exhibit commensurability ef-

fects at matching magnetic fields[15,18,21,22] and plastic flow phases which are not observed in random pinning conditions.[16,17] However, most importantly for us, periodic pinning is capable of restoring the coherence in current driven vortex motion even in relatively large macrobridges, resulting in appearance of Josephson-like effects in such structures.[4,9,10]

The physics of Josephson-like effects surfaced again as an utmost important issue in the context of high-T_c superconductors. High-T_c Josephson junctions cannot be fabricated with techniques developed for classical low-T_c Josephson elements. The ceramic nature of HTSC materials excludes the possibility of obtaining classical sandwich-type Josephson tunnel junctions, while extremely short coherence length and strong deterioration of HTSC films in the patterning process prevent fabrication of Josephson weak links shorter than the coherence length. In this context, the system of coherently flowing Abrikosov vortices can offer an alternative solution for weak-link Josephson devices capable of operating at liquid-nitrogen temperatures. Moreover, Josephson-like effects may be employed as an efficient tool for probing high-T_c vortex matter dynamics in periodic pinning structures.

Investigations of vortex motion related Josephson-like effects were restricted, to our best knowledge, exclusively to studies of Shapiro steps resulting from interactions of coherently flowing vortices with externally applied ac signals. However, in periodic pinning conditions one may possibly see also self-induced current steps resulting from matching of the current dependent frequency vortex nucleation to any harmonics of the natural self-frequency of the system set by the time of flight of vortices across the period of the imposed potential structure.

In this paper we report on our investigations of current-driven vortex dynamics in magnetically imposed controllable and reversible periodic pinning in HTSC epitaxial $Y_1Ba_2Cu_3O_{7-\delta}$ (YBCO) thin films. We discuss experiments revealing the existence of self-induced Josephson-like effects, mechanisms leading to periodic pining conditions, and provide a theoretical picture describing the experimentally observed phenomena.

II. PERIODIC PINNING: THEORETICAL BACKGROUND

Several methods of introducing artificial periodic pinning to superconducting films have been reported in the literature. The far from complete list includes spatially ordered radiation defects, thickness and composition modulation, magnetic impurities, two-dimensional arrays of magnetic and nonmagnetic dots, and periodic holes arrangement.[6,10,15,19,20,23,24] Application of any of the known techniques causes irreversible changes in the properties of investigated samples. We have recently proposed a technique enabling one to introduce a reversible and controllable arbitrary weak pinning potential to superconducting specimens.[25] The technique relies on interactions between vortices and spatially nonhomogeneous magnetic-field pattern produced by magnetic recording tape, containing a preregistered signal. The tape is placed in a close contact with the surface of the superconducting specimen which in this way is cooled across the superconducting transition in spatially inhomogeneous magnetic field; see Fig. 1.

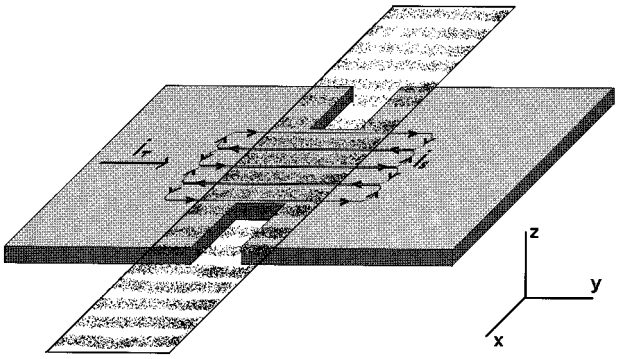

FIG. 1. Geometry of the superconducting macrobridge with the overlaying magnetic tape containing a prerecorded harmonic signal. Cooling of the sample in the presence of spatially periodic magnetic field of the tape results in the circulation of screening currents as indicated in the figure. For transport current I_t flowing in the y-direction vortices are flowing in the x direction, across the magnetically imposed periodic potential relief.

To evaluate the effect of the inhomogeneous field let us apply a magnetic tape containing a prerecorded harmonics signal to the surface of a flat superconducting specimen that occupies half space $z>0$. The recorded harmonic signal $s(t)=s_0\cos(\omega_s t)$ results in spatially periodic magnetic field $H_x=H_0\cos k_0 x$ at the tape-sample interface. The spatial periodicity of the field is simply $\lambda_m=2\pi u_r/\omega_s=2\pi/k_0$, where u_r is the speed of tape translation under the recording head. The profile of the magnetic field inside the superconductor can be obtained by solving London's equation, $\nabla^2\mathbf{H}-(1/\lambda_{eff}^2)\mathbf{H}=\mathbf{0}$, with the boundary condition $H_z(z=0)=H_0\cos k_0 x$. Here, $\lambda_{eff}=\lambda\coth(d/2\lambda)$ is the effective penetration depth of magnetic field into a superconducting flat specimen with the thickness d and λ is the London penetration depth. London's equation must be completed with Maxwell's equation for the free space, $\nabla\cdot\mathbf{H}=\mathbf{0}$. The solution for H_z reads

$$H_z(x,z)=H_0\cos(k_0x)\exp\left[-\sqrt{k_0^2+\frac{1}{\lambda_{eff}^2}}z\right]$$
$$=H_0\cos(k_0x)\exp(-\kappa z). \quad (1)$$

The energy of Abrikosov vortex located inside the considered specimen at the point x is

$$U=\int_0^d\frac{\Phi_0H_z}{4\pi}dz=\frac{\Phi_0H_0\cos k_0x}{4\pi\kappa}[1-\exp(-\kappa d)], \quad (2)$$

where Φ_0 is the flux quantum. Clearly, the application of a prerecorded magnetic tape imposes periodic potential on Abrikosov vortices moving in the superconductor. The force acting on a unit length of a vortex is

$$F=\frac{1}{d}(-\partial_x U)=\frac{\Phi_0H_0k_0}{4\pi\kappa d}[1-\exp(-\kappa d)]\sin(k_0x)$$
$$=F_0\sin(k_0x). \quad (3)$$

For currents flowing in the y direction and exceeding the critical depinning current the local vortex dynamics in mag-

netically imposed periodic potential relief will be governed by the following equation of motion:

$$\eta\dot{x}+F_0\sin(k_0x)=\frac{\Phi_0}{c}J_{ext}, \tag{4}$$

where η is viscosity per unit length of the vortex, $J_{ext}=(J-J_{c0})$, J is the density of external current, and J_{c0} is the density of the critical current in the absence of the periodic potential. We have assumed here that J_{ext} is independent of both x and z coordinates. Equation (4) can be rewritten using the reduced quantities

$$\dot{X}+b\sin X=a, \tag{5}$$

where $X=k_0x$ is the dimensionless coordinate of the position of the vortex bundle, $b=F_0k_0/\eta$ plays role of the force magnitude due to periodic magnetic modulation, and $a=J_{ext}\Phi_0k_0/(\eta c)$ stands for the reduced current density.

Equation (5), which is a well-known equation of motion for an overdamped pendulum, describes dynamics of many nonlinear systems, among them the classical weak link Josephson junction. The equation for the weak link follows straightforwardly from the resistively shunted junction model (RSJ) in the limit of small junction capacitance.[1] Our equation of motion is analytically solvable. By integrating Eq. (5) and taking the time derivative of the solution for $|\gamma|=|a|/b>1$ one obtains

$$\dot{X}_0(t)=\frac{\Omega^2a}{\left[\Omega\sin\left(\frac{\Omega t}{2}+\delta\right)-\gamma a\cos\left(\frac{\Omega t}{2}+\delta\right)\right]^2+a^2\cos^2\left(\frac{\Omega t}{2}+\delta\right)}, \tag{6}$$

where $\delta\in[0;2\pi]$ is an integration constant. The derivative of the obtained solution $\dot{X}_0(t)$ is periodic with the frequency $\Omega=\sqrt{a^2-b^2}$. The average vortex velocity $\langle\dot{X}\rangle$ can be calculated as a time average of Eq. (6):

$$\langle\dot{X}\rangle=\frac{\Omega}{2\pi}\int_0^{2\pi/\Omega}\dot{X}_0(t)dt=\Omega=\sqrt{a^2-b^2}. \tag{7}$$

Note that Eq. (7) is valid only for $|\gamma|>1$, since $\langle\dot{X}\rangle=0$ for $|\gamma|\leqslant 1$.

The electric field due to vortex motion $\vec{E}$ and the vortex velocity $\vec{v}$ are related by a simple, well-known equation $\vec{E}=-1/c(\vec{v}\times\vec{B})$. Since the electric field is constituted by additive contributions of all moving vortices, the mean total voltage due to vortex motion is thus given by the following formula:

$$\langle V\rangle=pn\frac{L\Phi_0}{c}\langle\dot{x}\rangle, \tag{8}$$

where L is a distance between the voltage measuring contacts, n is the density of flowing vortex bundles, and p is the number of vortices in a bundle. By rewriting this equation in reduced units we obtain an expression in a form of modified ac Josephson relation:

$$\langle V\rangle=pN\frac{\Phi_0\lambda_m}{2\pi cW}\langle\dot{X}\rangle=pN\frac{\hbar}{2e}\frac{\lambda_m}{W}\langle\dot{X}\rangle=ps\frac{\hbar}{2e}\Omega, \tag{9}$$

where W stands for the strip width and N is the total number of vortex bundles in the sample. In Eq. (9) we have introduced a quantity, the filling factor $s=N(\lambda_m/W)$, measuring the number of vortex bundles per each period of the imposed potential.

We conclude that placing the prerecorded magnetic tape on the sample surface results in penetration of spatially periodic field pattern into a superconducting specimen. The pattern reproduces the shape of the prerecorded signal and thus determines the spatially periodic potential relief in the sample. The vortex dynamics is now governed by the equation of motion which is equivalent to the phase equation for the low-capacitance classical Josephson junctions.

The latter system is known to exhibit dc current Shapiro steps on the I-V curves of junctions irradiated with microwave signals[1,26–30]. The positions of these steps are determined by the frequency of the incident radiation via the famous Josephson relation:

$$V_n=n\frac{\hbar}{2e}\omega_{ext}. \tag{10}$$

Shapiro steps are traditionally regarded as a hallmark of the presence of ac Josephson effects in the investigated system. However, as it has been widely discussed in the literature, similar current steps will appear when a system of coherently moving vortices locks to the externally applied ac signal.[2–10] In the system of coherently flowing vortices the role of the Josephson frequency is played by the frequency of vortex creation at the sample borders. Since each vortex carries magnetic flux quanta $\Phi_0=hc/2e$, the voltages at which dc current steps show out in the I-V curve of coherently flowing vortex system are related to the external frequency through the same Josephson relation, see, e.g., Ref. 6.

In the following we shall demonstrate that coherent vortex motion in periodic magnetic structures gives rise to natural characteristic frequencies of the vortex system. Locking of this frequency to any harmonics of the frequency at which vortices are nucleated at the strip borders leads to resonant solutions of the relevant equation of motion and appearance of self-induced Shapiro-like steps on the I-V characteristics, even in the absence of any external ac signal.

III. PERIODIC PINNING: EXPERIMENTAL

Magnetically enforced artificial periodic pinning structures should have the most pronounced influence on vortex

and transport properties in good quality films with low intrinsic disorder. We have performed our experiments using thin film macrobridges fabricated from highly oriented high-T_c $Y_1Ba_2Cu_3O_{7-\delta}$ thin films deposited by two techniques; laser ablation,[31] or alternatively, sputtering in high-pressure dc inverted cylindrical magnetron configuration.[32]

Sputtered films were deposited on single-crystal (100) $LaAlO_3$ substrates while the laser ablated films were grown on (100) MgO and $SrTiO_3$ crystals. The substrates were *in situ* oxygenated before the film deposition by a 30-min-long oxygen fast ion bombardment at 630° C. The magnetron films were grown in a 4:3 atmosphere of Ar and O_2 at a total pressure of 95 Pa, and substrate temperature of 790° C. In order to obtain smooth and good quality $Y_1|Ba_2Cu_3O_{7-\delta}$ films the magnetron power was modulated during the deposition process by controlling the plasma ion current.[32] The laser ablated films were grown in oxygen pressure of 0.3 mbar using 308-nm XeCl excimer laser pulses with energy around 100 mJ per pulse. After deposition the samples were slowly cooled down in oxygen atmosphere at a pressure of 800 mbar and no further processing was needed. Typical rate of deposition of the sputtered films was 0.5 Å/s while that of the laser films was about 1.5 Å/s. Typical thickness ranged from 50–100 nm for the sputtered films and from 200–300 nm for laser ablated films.

As-deposited films were patterned by means of standard photolithography and chemical etching into macrobridge geometry with a four-contact arrangement for transport measurements. The macrobridge constrictions had widths ranging from 50–250 μm and lengths from 10–50 μm. The constriction increases locally the density of transport current and thus localizes spots where vortices may nucleate. The contact pads were additionally covered with vacuum deposited silver overlay enabling thermal bonding of contact wires.

Patterned samples were selected by choosing those with the highest value of the residual resistance ratio R_{300K}/R_{100K}. This criterion allowed us to select films with lowest intrinsic disorder pinning in which magnetically applied pinning structures should have the most pronounced effect on transport properties.

Spatially periodic magnetic structures were formed by recording periodic signals on magnetic tape, using a recorder with a narrow slit in the recording head. The period of the pinning structure, created by recording a single frequency harmonic signal, is determined by the signal frequency and recording speed. We have used the standard recording speed of 4.8 cm/s. The grain size of the ferromagnetic tape material and the width of the slit in the recording head set the spatial resolution limit for the magnetically imposed pinning. The same factors determine the upper frequency bandwidth of a tape recorder. In our case, the bandwidth limit sets the shortest period available using this technique to be of the order of 3 μm. In the experiments, the piece of the magnetic tape containing a preregistered signal has been placed directly on the top of the strip and pressed into a close contact with the surface by means of phosphor-bronze flat spring. The orientation of magnetic tape is such that transport current will force vortices to flow across the periodic potential structures. The entire arrangement of the superconducting strip and the tape has been thermally anchored to a sample holder of mu-metal screened variable-temperature cryostat.

Since in the experiments we have not applied any external magnetic field the entire vortex dissipation is due to the flow of vortices created by the self-field of the transport current. This type of dissipation is known to be associated with channeled flow of multiquanta bundles of vortices flowing in spontaneously created channels of easy vortex flow.

The application of a tape containing a pre-recorded periodic signal visibly modifies conditions for vortex motion in the sample. As we have recently reported in details elsewhere[25] the application of the tape modifies the current of the dissipation onset in the strip, brings about commensurability effects that have been observed in the sample magnetoresistance measured at a constant current flow, and enforces the coherence in the current-driven vortex motion.

The evidence for the coherent nature of vortex motion in magnetic periodic potential comes from detailed analysis of the strip I-V curves, recorded after application of the magnetic tape. The initial low-voltage part of the I-V characteristics shows series of current steps closely resembling Shapiro steps on I-V curves of microwave irradiated classical Josephson junctions. We have shown an example of a pronounced step structure in Fig. 7 of our recent paper.[25] Observe that in the reported experiments no external ac signal has been applied to the sample. The step structure results, as will be discussed in details below, from resonant locking of the self-induced frequencies of the coherently flowing vortex system to the frequency of vortex nucleation at the strip edge. The self-induced ac signal is generally very weak. Therefore the induced step amplitudes are very low, vulnerable to thermal and electromagnetic noise smearing. For this reasons, in order to proceed with the detailed analysis of the step structure we have not used directly the I-V recordings but rather the dV/dI vs V characteristics measured by means of the lock-in technique. To remove any possible randomness in the registered curves we have typically averaged several recordings before proceeding with the analysis. Voltage positions of Josephson-like current steps are marked by sharp minima in thus measured derivative characteristics; see, e.g., Fig. 6 in Ref. 25. Let us underline that we have carefully verified that the minima due to the step structure were rigorously absent in the derivative characteristics measured without any magnetic tape.

IV. SELF-INDUCED STEPS: THEORETICAL PICTURE

When bundles of current-created vortices penetrate the sample an additional alternating current component proportional to dN/dt appears in the system. Let us assume that the nucleation process occurs with some frequency $\omega_0 = 2\pi/T$. In the following we shall demonstrate that the resonant effects occur when the frequency Ω of the moving vortex system coincides with any of the harmonics $n\omega_0$ of the self-ac signal generated by vortex nucleation process. The equation of motion accounting for such ac excitation becomes

$$\dot{X} + b \sin X = a + Af(t). \tag{11}$$

Unfortunately, the equation of motion containing time-dependent driving term cannot be solved analytically. Equation (5) with sinusoidal driving term has been solved in the context of Josephson junctions by analog computing methods.[26] However, here we can take advantage of the fact that self-induced ac signals are very weak and will consider them as a small perturbation to the total current. We proceed with calculations by expanding X into power series of a small perturbation parameter $\varepsilon = A, X = \Sigma_{i=0}^{\infty} X_i \varepsilon^i$. In order to avoid unphysical divergence we must likewise expand the driving term a into perturbation series of the same parameter $a = \Sigma_{i=0}^{\infty} a_i \varepsilon^i$. Restricting ourselves to the first-order terms we have

$$\dot{X}_0 + b \sin X_0 = a_0, \tag{12}$$

$$\dot{X}_1 + b\dot{X}_1 \cos X_0 = a_1 + f(t). \tag{13}$$

The perturbation solution to Eq. (13) can be obtained using the formalism which one of us described in detail in Ref. 33. Introducing the phase shift δ relative to the frequency in the definition of $f(t)$ we obtain a first-order correction term to the reduced current density,

$$a_1 = \frac{b}{a_0} \langle f(t) \cos(\Omega t + \delta) \rangle. \tag{14}$$

Since the process of vortex bundles nucleation is periodic in time we can expand $f(t)$ in Fourier series. Assuming for simplicity that $f(t)$ is an even function we write

$$f(t) = \sum_{n=0}^{\infty} f_n \cos(n\omega_0 t). \tag{15}$$

Calculating the average (14) we find that it differs from zero only at currents at which $\Omega = \Omega_n \equiv n\omega_0$. The nonzero resonant dc current component,

$$a_1 = \frac{b}{a_0} \sum_{n=0}^{\infty} f_n \langle \cos(n\omega_0 t) \cos(\Omega t + \delta) \rangle = \frac{b}{2a_{ext}} f_n \cos\delta, \tag{16}$$

is added or subtracted from the total dc transport current, depending on the phase δ, thus giving rise to the series of current steps with the height of the nth step $(\Delta a_1)_n = (b/a_{ext}) f_n$.

Resonant self-induced current steps on the I-V curve appear at voltages V_n which are given by the modified Josephson relation (9) for the resonant frequencies $\Omega = \Omega_n = n\omega_0 = \sqrt{a_{rn}^2 - b^2}$. Expressing thus obtained step voltages in nonreduced units we have

$$V_n = ps \frac{\hbar}{2e} \frac{\Phi_0 J_{rn}}{\eta c} k_0 \sqrt{1 - \left[\frac{cH_0 k_0}{4\pi J_{rn} \kappa d} [1 - \exp(-\kappa d)] \right]^2}, \tag{17}$$

where the resonant current $J_{rn} = 2e/h \sqrt{(n\omega_0 \eta / k_0)^2 + F_0^2}$.

The expression for voltages at which self-induced current steps appear on the I-V curve can be simplified for different physical situations. In particular, in our experiments $\kappa d \sim 1$ and

$$V_n = ps \frac{\hbar}{2e} \frac{\Phi_0 J_{rn}}{\eta c} k_0 \sqrt{1 - \left[0.63 \frac{cH_0 k_0}{4\pi J_{rn}} \right]^2}. \tag{18}$$

V. DISCUSSION

One should immediately stress the clear difference between Shapiro-like steps induced by irradiating the system of coherently flowing vortices with external microwave signal and the discussed case of self-induced vortex current steps. The former steps are equidistant and voltage separation between them is given by the Josephson relation (10). In a marked difference, the voltages at which the resonant condition $\Omega = \Omega_n$ is fulfilled depend on the current flow. Current dependence appears in Eq. (17) both directly and through current dependence of the filling factor s. The distance between adjacent self-induced current steps depends therefore on the current flow, i.e., on the step number. For this reason we limit our present analysis to the voltages at which the first steps appear.

The first step appears at the I-V characteristics for the lowest possible filling factor $s = N(\lambda_m / W)$. In a symmetric strip geometry, like the one used in the experiments where probabilities of nucleation of vortex and antivortex bundles on the opposite edges of the strip are equal, the lowest possible filling factor is $s = 2(\lambda_m / W)$. Putting this value into Eq. (18) we obtain the voltage position of the first step:

$$V_{1s} = p \frac{\hbar}{2e} \frac{\Phi_0 J_{rs1}}{\eta c} \frac{2\pi}{W} \sqrt{1 - \left[0.63 \frac{cH_0 k_0}{4\pi J_{rs1}} \right]^2}. \tag{19}$$

The physics involved in the step structure becomes immediately transparent when one considers the first step voltage in the experimentally realistic approximation of small k_0 and H_0, such that $0.63(cH_0 k_0 / 4\pi J_{rn})^2 \ll 1$. Within this approximation we get from Eq. (19)

$$V_{1s} \approx p \frac{h}{2e} \frac{\Phi_0 J_{rs1}}{\eta c} \frac{2}{W} = p \frac{h}{2e} v(J_{rs1}) \frac{2}{W} = p \frac{\hbar}{2e} \omega_{W/2}, \tag{20}$$

where v is the vortex velocity and $\omega_{W/2}$ is a natural self-frequency of the system set by the time of flight of current driven vortex bundles across the half-width of the strip. The first self-induced step corresponds therefore to the locking of the vortex nucleation frequency to the frequency set by the inverse of the lifetime of a bundle in the strip, i.e., to the time of flight across the half-width of the strip. Subsequent steps occur for higher harmonics of this frequency. Due to the fact that the filling factor for the current flow corresponding to the voltage of the first step is $s < 1$, we shall refer to this step as to the first subharmonic self-induced vortex step.

Schematic representation of the vortex scenario leading to the appearance of the first two subharmonic steps is illustrated in Fig. 2. In the figure we illustrate the periodic potential which is commensurable with the sample width. Observe that in the experimental reality $W \gg \lambda_m$ and the ratio $W/2\lambda_m$ can be with a reasonable accuracy always approximated by an integer number. In Fig. 2 for the sake of simplicity we show relatively low ratio $W/\lambda_m = 20$. Vortices nucleate at the bottom edge of the strip and flow up to the middle of the strip where they annihilate with antivortices nucleated with

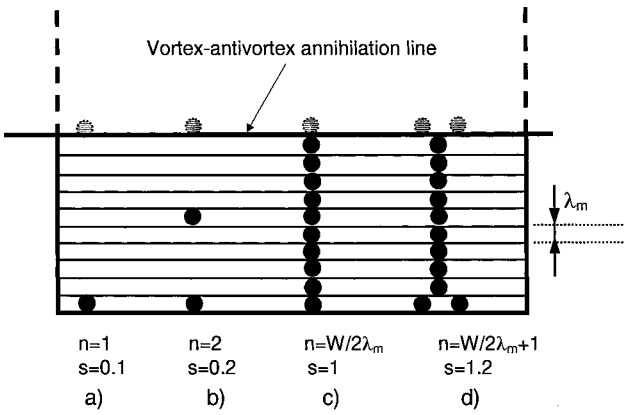

FIG. 2. The vortex scenarios leading to appearance of the first and second subharmonic step are shown in (a) and (b), respectively. The generation of the first harmonic step is illustrated in (c). Splitting of the easy vortex flow channel when surpassing the first harmonic step and abrupt doubling of the voltages of the subsequent subharmonic steps is shown in (d). Only half of the sample width, from the edge up to the vortex-antivortex annihilation line, is shown in the figure.

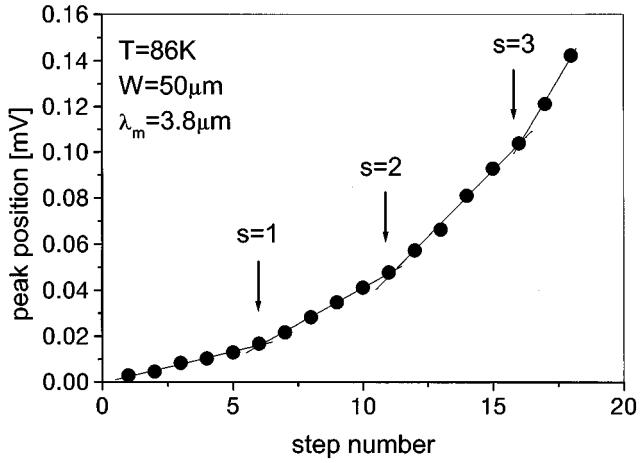

FIG. 3. Step voltage as a function of the step number. Note the change in the slope of the dependence at the points corresponding to harmonic steps, where the filling factor $s=n, n=1,2,3,\ldots$, indicates that in average at bias points of the harmonic steps all potential minima are filled with vortex bundles and accommodation of an additional one leads to splitting of the existing easy vortex flow channels and doubling of the filling factor for the next subharmonic steps, see the schematics shown in Fig. 4(d). The doubling of the filling factor leads to abrupt doubling of the voltages of the subsequent subharmonic steps.

the same rate at the opposite (not shown) edge of the strip. In the case labeled (a) the frequency of nucleation of vortices locks to the time of flight across the half-width of the bridge. These are the bias conditions leading to the appearance of the first subharmonic step. In case (b) the second harmonics of the nucleation frequency locks to the time of flight and the second subharmonic step appears. At these bias conditions we have two vortex bundles and two antivortex bundles that simultaneously and coherently flow across the bridge.

With increasing step number, i.e., with increasing transport current, the number of bundles simultaneously flowing in a channel increases. At the bias point corresponding to the step with number n equal to the maximum integer of the ratio $W/2\lambda_m$ the vortex nucleation frequency is locked to the time of flight between two adjacent minima of the magnetic period. This situation is schematically illustrated in Fig. 2(c). At bias conditions of the step $n=W/2\lambda_m$, in the approximation of commensurability of the magnetic period with the sample width or in the case $W \ll \lambda_m$, all potential minima are occupied by flowing vortices and $s=1$.

The step at which the filling factor $s=1$ will be referred to as the first harmonic step. The voltage of this step is

$$V_1 = p\frac{\hbar}{2e}\frac{\Phi_0 J_{1n}}{\eta c}k_0\sqrt{1-\left[0.63\frac{cH_0k_0}{4\pi J_{r1}}\right]^2}. \qquad (21)$$

Again, in the approximation of large λ_m and weak modulating field we have

$$V_1 \approx p\frac{h}{2e}\frac{\Phi_0 J_{1n}}{\eta c}\frac{1}{\lambda_m} = p\frac{\hbar}{2e}\omega_\lambda, \qquad (22)$$

where ω_λ is yet another self-frequency of the system, this time set by the time of flight across the magnetic period.

Any further increase of the bias current beyond the point corresponding to the step number $W/2\lambda_m$, where $s=1$ and all potential minima in the chain are already occupied by vortex bundles, will cause the splitting of the vortex channel. It is energetically more favorable for the next entering bundle to split the channel rather than to squeeze itself into the existing fully loaded vortex chain; see Fig. 2(c). Splitting of the channel results in doubling of the number of nucleating vortices that will simultaneously lock to time of flight across the characteristics length $W/2$. The increase in the number of coherently flowing vortices is formally reflected in the doubling of the filling factor for the subsequent subharmonic steps. Therefore the voltages of the next subharmonic steps appearing after the channel splitting will be abruptly increased with respect to those seen before the splitting instability, as illustrated in Fig. 2(d).

Obviously, the subharmonic step with the number $n=W/2\lambda_m$ will coincide with the first harmonic step. Experimentally one can distinguish the harmonic steps from the subharmonic ones as the steps at which the voltage separation between the subsequent steps abruptly doubles. This can be done by analyzing the plot of the step voltages as a function of the step number as shown in Fig. 3. One can easily see the hallmarks of three splitting instabilities in the coherently flowing vortex system, marked by a sharp change of the slope of the presented data. The instabilities occur at the steps with an integer value of the filling factor s. These steps can be thus identified as the consecutive harmonic steps.

It is worthwhile reminding here that in early experiments with microwave induced vortex steps in periodically corrugated superconducting films Martinolli noted that steps appear only at magnetic fields corresponding to the matching field, i.e., at the fields for which the periodicity of the vortex lattice matches the period of the thickness modulation of the employed films.[6] The matching field condition corresponds directly to the filling factor $s=1$ for the case of vortices created by self-field of the current only. Indeed, for $s=1$ each potential well is filled with a vortex bundle.

The above-performed analysis brings us to the conclusion that the voltages at which the first subharmonic step appears

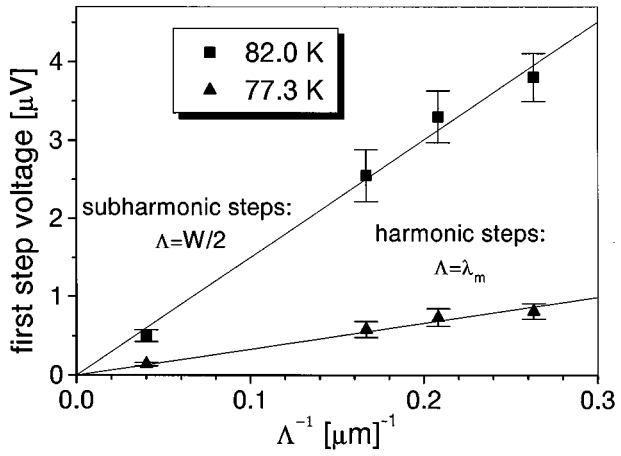

FIG. 4. Voltage positions of the first self-induced current steps as a function of inverse of a characteristic length Λ which is the inverse of spatial magnetic period for the harmonic steps and of half-width of the sample for the subharmonic steps. Data were obtained from the positions of minima in the averaged dV/dI vs I curves recorded for the same strip at two different temperatures with tapes of different spatial periodicity of the prerecorded signal. The continuous lines represent the best fit to the linear dependence.

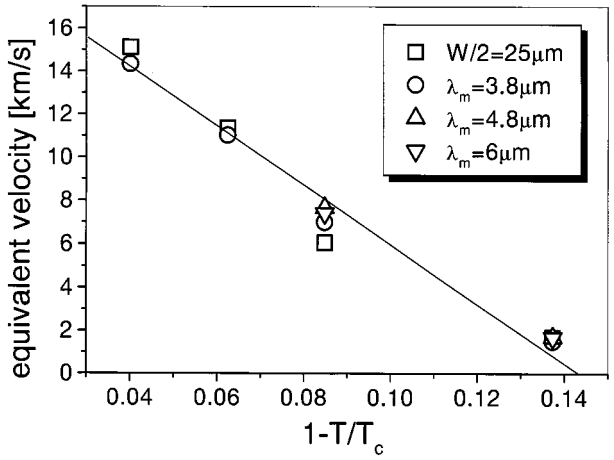

FIG. 5. Equivalent vortex flow velocity as a function of temperature. The equivalent velocity is the velocity calculated from the experimentally determined first steps voltages by assuming that the voltage is due to the coherent motion of a single vortex ($p=1$) only. The real vortex velocities are orders of magnitude lower since vortices move in large flux bundles, $p \ll 1$. Note that the temperature axis is scaled as $1-T/T_c$.

should scale inversely proportional to the sample half-width, see Eq. (20), while the positions of the first harmonic steps should scale with the inverse of magnetic period with the same proportionality coefficient, see Eq. (22). In order to check this prediction we have investigated in detail the voltages at which the first harmonic and subharmonic steps appear. Measurements were executed using the same strip and changing the applied magnetic field pattern by using recordings with different spatial periodicity. In Fig. 4 we show, for two different temperatures, the dependence of the voltage of the first current step on the inverse of a characteristic length scale Λ, where $\Lambda = W/2$ for subharmonic steps and $\Lambda = \lambda_m$ for harmonic ones. The data in Fig. 4 fall on straight lines and demonstrate that the experimental results are consistent with the model predictions. The decrease of the slope of linear fits to the data in Fig. 4 with decreasing temperature can be ascribed to the decrease of vortex flow velocity due to the increasing viscosity. The temperature dependence of the first step voltages can be thus presented in the terms of the temperature dependence of equivalent vortex velocity, i.e., velocity ''per single vortex,'' calculated from Eqs. (22) and (20) by putting $p=1$. This is presented in Fig. 5 using different symbols for data taken with different magnetic periods. The data in Fig. 5 is plotted against x axis scaled as $1-T/T_c$, where T is the temperature and T_c is the critical temperature, i.e., scaled according to the expected temperature dependence of the viscosity factor in the temperature range of the experiment. The data plotted in this manner can be well fitted with a linear dependence, confirming again that the temperature dependence of the step voltage is due to the temperature changes in the viscosity factor.

However, thus obtained equivalent vortex velocity is orders of magnitude higher than the one realistically expected in the experiment. Let us remind the reader that we have calculated the equivalent vortex velocities under the assumption of $p=1$, i.e., assuming motion of a single vortex. Nevertheless, as it was already pointed out earlier, in the current driven dissipative vortex motion vortices move in bundles containing large number of flux quanta and not as single vortices. This brings us to the problem of the actual size of the moving vortex bundle.

The size of moving vortex bundles, i.e., number of vortices in a bundle p, can be estimated from the equivalent vortex velocity. Assuming that the viscosity of the superconductor is of the order of typical vortex viscosity reported in the literature, $\eta \propto 10^{-6}-10^{-7}$ cgs units,[34] the resulting bundle size is of the order of $p \propto 10^3-10^4$. Otherwise, for $p \sim 1$ we would have to assume that the viscosity is very low, much below the standard values for YBCO, say of the order of $\eta \propto 10^{-12}$ cgs units.

The viscosity issue has been already discussed in the literature, cf. Refs. 9,35,34. Many authors have observed apparently low vortex viscosity in dc current induced vortex motion and ascribed that fact to Josephson vortices, known to have viscosity coefficient several orders of magnitude lower than the Abrikosov vortices.[36] However, it is hard to imagine the presence of Josephson vortices in good quality films as those used in the experiments. In fact, the literature does not provide direct experimental confirmation of the Josephson vortex hypothesis.

Yet another explanation for very low viscosity invokes the nonequilibrium phenomena occurring at high velocities of the vortex motion.[37] However, the onset of nonequilibrium vortex motion should be clearly marked by the voltage jump in the I-V characteristics, a feature that has not been observed by us in the experiments.

We believe that the most plausible explanation is the huge size of moving bundles. The number of vortices in a bundle p becomes a multiplicative factor in the voltage scale. The physical reality of this concept has been demonstrated already in the early experiments on flux flow noise in classical superconductors; see Ref. 38 for a review. Voltage noise associated with flux motion has been also used to estimate the size of moving vortex bundles in high-T_c superconducting thin films. The bundle size of the order of 10^3-10^4 vor-

tices has been found from the analysis of random telegraph voltage fluctuations in current driven thin BSCCO films where the telegraph noise voltage was found to be due to the intermittence in the motion of flux bundles.[39] Recently published analysis of low-frequency voltage noise spectra in epitaxial YBCO thin films concludes that at liquid-nitrogen temperatures vortices move in bundles containing an equivalent number of about 10^4 flux quanta.[40] Therefore we conclude that the huge size of flowing flux bundles estimated in the reported experiments from the self-induced step voltages is consistent with flux bundle sizes that were observed in other experiments involving high-T_c thin films.

ACKNOWLEDGMENT

This work was supported by The Israel Science Foundation founded by The Academy of Sciences and Humanities, Israeli Ministry of Science, and National Research Council of Italy in the framework of the Research and Training program for Third Mediterranean Countries.

*Also at Instytut Fizyki PAN, Al. Lotników 32, PL 02-668 Warszawa, Poland.

[1] A. Barone and G. Paterno, *Physics and Applications of the Josephson Effect* (John Wiley and Sons, New York, 1982).

[2] K.K. Likhariev, Zh. Éksp. Teor. Fiz. **61**, 1700 (1971) [Sov. Phys. JETP **34**, 906 (1972)].

[3] L.G. Aslamasov and A. Larkin, Zh. Éksp. Teor. Fiz. **68**, 766 (1975) [Sov. Phys. JETP **41**, 381 (1975)].

[4] A.A. Lykov, Usp. Fiz. Nak **164** (10), 1 (1992) [Sov. Phys. Usp. **35**, 811 (1992)].

[5] V.N. Gubankov, V.P. Koshelec, and G.A. Ovsyannikov, Zh. Éksp. Teor. Fiz. **71**, 348 (1976) [Sov. Phys. JETP **44**, 181 (1976)].

[6] P. Martinoli, Phys. Rev. B **17**, 1175 (1978).

[7] C. Camerlingo, G. Jung, M. Cerdonio, C. Tosello, and S. Vitale, in *SQUID '85*, edited by H.D. Hahlbohn and H. Lubbig (Walter de Gruyter, Berlin, 1985), p. 665; C. Camerlingo, G. Jung, M. Cerdonio, S. Vitale, and C. Tosello, in *Weak Superconductivity*, edited by A. Barone and A. Larkin, Progress in High Temperature Superconductivity Vol. 4 (World Scientific, Singapore, 1987), pp. 293-303.

[8] H. Rogalla and C. Heiden, in *Superconducting Quantum Electronics*, edited by V. Kose (Springer-Verlag, Berlin, 1991), pp. 80–127.

[9] M.J.M.E.P. de Nivelle, G.J. Gerritsma, and H. Rogala, Physica C **233**, 185 (1994).

[10] P. Martinoli, O. Daldini, C. Leemann, and B. van derBrandt, Phys. Rev. Lett. **36**, 382 (1976).

[11] G. Jung, J. Konopka, P. Gierlowski, and W. Kula, Appl. Phys. Lett. **54**, 2355 (1989); G. Jung and J. Konopka, Europhys. Lett. **10**, 183 (1989).

[12] G.A. Ovsyannikov, Z.G. Ivanov, J. Mygind, and N.F. Pedersen, Physica C **241**, 228 (1995).

[13] G. Blatter, M.V. Feigelman, V.B. Geshkenbein, A.I. Larkin, and V.M. Vinokur, Rev. Mod. Phys. **66**, 1125 (1994); G.W. Crabtree and D.R. Nelson, Phys. Today **38** (4), 38 (1997).

[14] B.Y. Zhu, Jinming Dong, and D.Y. Xing, Phys. Rev. B **57**, 5063 (1998).

[15] Y. Jaccard, J.I. Martin, M.-C. Cyrille, M. Velez, J.L. Vicent, and Ivan Shuller, Phys. Rev. B **58**, 8232 (1998).

[16] C. Reichhardt, C.J. Olson, and Franco Nori, Phys. Rev. Lett. **78**, 2648 (1997); Phys. Rev. B **58**, 6434 (1998).

[17] C. Reichhardt, J. Groth, C.J. Olson, S.B. Field, and F. Nori, Phys. Rev. B **54**, 16 108 (1996).

[18] C. Reichhardt, C.J. Olson, and Franco Nori, Phys. Rev. B **57**, 7937 (1998).

[19] J.-Y. Lin, M. Gurevitch, S.K. Tolpygo, A. Bourdillon, S.Y. Hou, and J.M. Phillips, Phys. Rev. B **54**, R12 717 (1996).

[20] Y. Otani, B. Pannetier, J.P. Nozieres, and D. Givord, J. Magn. Magn. Mater. **126**, 622 (1993); J.I. Martin, M. Velez, J. Nogues, and I. Schuller, Phys. Rev. Lett. **79**, 1929 (1997).

[21] C. Reichhardt and F. Nori, Phys. Rev. Lett. **82**, 414 (1999).

[22] D.D. Morrison and R.M. Rose, Phys. Rev. Lett. **25**, 356 (1970).

[23] A.T. Fiory, A.F. Hebard, and S. Somekh, Appl. Phys. Lett. **32**, 73 (1978).

[24] A. Pruijboom, E. van der Druft, and P.H. Kes, Physica C **165**, 179 (1990).

[25] Y. Yuzhelevski and G. Jung, Physica C **314**, 163 (1999).

[26] P. Russer, J. Appl. Phys. **43**, 2008 (1972).

[27] H. Kanter and F.L. Vernon, J. Appl. Phys. **43**, 3174 (1972).

[28] L.G. Aslamasov and A.I. Larkin, Zh. Eksp. Teor. Fiz., Pis'ma Red. **9**, 150 (1969) [JETP Lett. **9**, 87 (1969)].

[29] M. Kvale and S.E. Hebboul, Phys. Rev. B **43**, 3720 (1991).

[30] M. Kvale, S.E. Hebboul, and J.C. Garland, Physica B **165-166**, 1585 (1990).

[31] M. Guilloux-Viry, C. Thivet, M.G. Karkut, J. Padiou, O. Peña, A. Perrin, M. Sergent, and A. Gauneau, Mater. Sci. Eng. B **18**, 115 (1993).

[32] C. Camerlingo, B. Ruggiero, M. Russo, E. Sarnelli, A. Del Vecchio, F. De Riccardis, and L. Tapfer, J. Alloys Compd. **251**, 34 (1997).

[33] B.Ya. Shapiro, M. Gitterman, I. Dayan, and G.W. Weiss, Phys. Rev. B **46**, 8416 (1993).

[34] M. Golosovsky, M. Tsendlikht, and D. Davidov, Supercond. Sci. Technol. **9**, 1 (1996), and references therein.

[35] M.J.M.E. de Nivelle, W.A.M. Aarnik, M.V. Pedyash, E.M.C.M. Reuvekamp, D. Trepstra, M.A.J. Verhoeven, P.J. Gerritsma, and H. Rogalla, IEEE Trans. Appl. Supercond. **3**, 2512 (1993).

[36] A.M. Portis and K.W. Blazey, Solid State Commun. **68**, 1097 (1988).

[37] S.G. Doettinger, R.P. Huebener, R. Gerderman, A. Kühle, S. Anders, T.G. Träuble, and J.C. Villegier, Phys. Rev. Lett. **73**, 1691 (1994).

[38] John R. Clem, Phys. Rep. **75**, 1 (1981).

[39] G. Jung, Y. Yuzhelevski, B. Savo, C. Coccorese, V.D. Ashkenazy, and B.Ya. Shapiro, in *Unsolved Problems of Noise*, edited by Ch.R. Doering, L. Kiss, and M.F. Shlesinger (World Scientific, Singapore, 1997), p. 285.

[40] K.E. Gray, Phys. Rev. B **57**, 5524 (1998).